Bioresource Technology 300 (2020) 122634

Contents lists available at ScienceDirect

Bioresource Technology

journal homepage: www.elsevier.com/locate/biortech

Sequential vertical flow trickling filter and horizontal flow multi-soil-layering reactor for treatment of decentralized domestic wastewater with sodium dodecyl benzene sulfonate

Wenchang Tang[a,b,1], Xiang Li[a,1], Haiyang Liu[c,1], Shaohua Wu[a], Qi Zhou[a], Cheng Du[b], Qing Teng[b], Yuanyuan Zhong[b], Chunping Yang[a,b,d,*]

[a] College of Environmental Science and Engineering, Hunan University, and Key Laboratory of Environmental Biology and Pollution Control (Hunan University), Ministry of Education, Changsha, Hunan 410082, China
[b] Guangdong Provincial Key Laboratory of Petrochemcial Pollution Processes and Control, School of Environmental Science and Engineering, Guangdong University of Petrochemical Technology, Maoming, Guangdong 525000, China
[c] Datang Environment Industry Group Co., Ltd. Beijing 100097, China
[d] Hunan Provincial Environmental Protection Engineering Center for Organic Pollution Control of Urban Water and Wastewater, Changsha, Hunan 410001, China

GRAPHICAL ABSTRACT

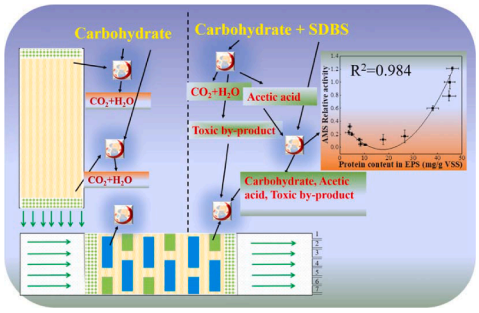

ARTICLE INFO

Keywords:
Multi-soil-layering
Trickling filter
EPS
Domestic wastewater
Surfactant

ABSTRACT

Sequential vertical flow trickling filter and horizontal flow multi-soil-layering bioreactor were investigated for the treatment of decentralized domestic wastewater at various concentrations of sodium dodecyl benzene sulfonate (SDBS). Results have shown that the removal rate of COD could reach 92.1% at initial COD concentration of 960 mg/L (800 mg/L was provided by SDBS). NH_4^+-N concentration could be reduced from 52.4 to 9.71 mg/L without aeration. Besides, a quadratic function model was fit to describe the relationship between the relative activity of amylase and the protein content in extracellular polymer substance. SDBS could inhibit the transport and metabolisms of amino acids, lipids and carbohydrates in biofilms. The analysis of three-dimensional fluorescence diagram indicated that the peak in excitation/emission wavelengths = 310–340/370–430 nm was the characteristic peaks of some active substances such as some enzymes in EPS. Only *Microbacterium* could totally offset the toxicity of SDBS degradation products.

* Corresponding author at: College of Environmental Science and Engineering, Hunan University, and Key Laboratory of Environmental Biology and Pollution Control (Hunan University), Ministry of Education, Changsha, Hunan 410082, China.
E-mail address: yangc@hnu.edu.cn (C. Yang).
[1] These authors contribute equally to this paper.

https://doi.org/10.1016/j.biortech.2019.122634
Received 31 October 2019; Received in revised form 12 December 2019; Accepted 15 December 2019
Available online 17 December 2019
0960-8524/

1. Introduction

Domestic wastewater pollution in rural China has become a serious environmental challenge because of lacking applicable wastewater management (He et al., 2016). In the last two decades, treatment of decentralized domestic wastewater in the rural areas has attracted increasing attention (Lin et al., 2019; Wang et al., 2011). In general, decentralized wastewater treatment methods include sand filter, septic tank and constructed wetland (Luo et al., 2014; Zhou et al., 2018). However, these treatment systems often require large land area. To address the challenge, new technologies for decentralized wastewater treatment have been developed in recent years, including downflow hanging sponge reactor (Bundy et al. 2017), horizontal constructed wetland (Fountoulakis et al., 2017), duckweed and water grass-based aquatic system (Zhou et al., 2019; Cheng and Stomp, 2009). A common deficiency of these technologies is that only small amount of wastewater was treated (Oakley et al., 2010; Lin et al., 2019b). Thus, there is a great demand to develop effective treatment of large amount rural wastewater.

Soil-based wastewater treatment technologies have been extensively used for decentralized wastewater disposal due to their high treatment capacity, low cost and readily availability of microbial communities (Bezbaruah et al., 2010; Oakley et al., 2010; Zhang et al., 2015a). However, there are serious practical problems with the conventional soil-based systems, including clogging, large footprint and low hydraulic loading rate (Li et al., 2018; Pant and Adholeya, 2009). Multi-soil-layering (MSL) biofilter, an emerging technology, has been widely used in the treatment of rural domestic wastewater. For example, Luo et al. (2014) invented a two-stage vertical hybrid system including a trickling filter and an MSL reactor to treat simulated septic tank effluent, which exhibited high treatment performance. The removal rate efficiencies of chemical oxygen demand (COD), NH_4^+-N and total phosphorus (TP) were 93.1%, 86.3% and 93.2%, respectively. Zhang et al. (2015a) had developed a trickling filter with an alternative MSL, which is comprised of soil mixed blocks (SMB) surrounded by permeable layers (PL). Pant and Adholeya (2009) proposed anaerobically digested wastewater from a cane molasses-based distillery through a two-stage sequential treatment, which could remove 84% nitrogen. But these did not address the harm of surfactants to the system.

Sodium dodecyl benzene sulfonate (SDBS) is an anionic surfactant widely used in Chinese countryside, and as a result, wastewater usually contains high concentrations of surfactants (He et al., 2017; Yang et al., 2018; Wu et al., 2018a). SDBS has toxic and bioaccumulation effect on many aquatic plants, fish and microorganisms (Parhizgar et al., 2017; Wu and Li, 2002; Zhang et al., 2015). Asok et al. (2012), Perez et al. (2016), Perez-Armendariz et al. (2010), Ying et al. (2002) reported that the average concentration of surfactant in domestic wastewater is about 200 mg/L, while this value can reach 500 mg/L in rural areas. At present, there are many technologies for removing SDBS, such as chitosan adsorption, aerobic treatment, and purification of *α-Proteobacterium* (Parhizgar et al., 2017; Perez-Armendariz et al., 2010; Wu and Li, 2002). However, researches on the removal of SDBS in the MSL system are lacking.

In this work, a novel two-stage system consisting of vertical flow trickling filter and horizontal flow multi-soil-layering reactor (VFTF-HFMSL) was studied to treat synthetic domestic wastewater with high SDBS of 750 mg/L. The removal efficiency of COD, NH_4^+-N, NO_3^--N and TP from the wastewater were discussed. In addition, the changes of

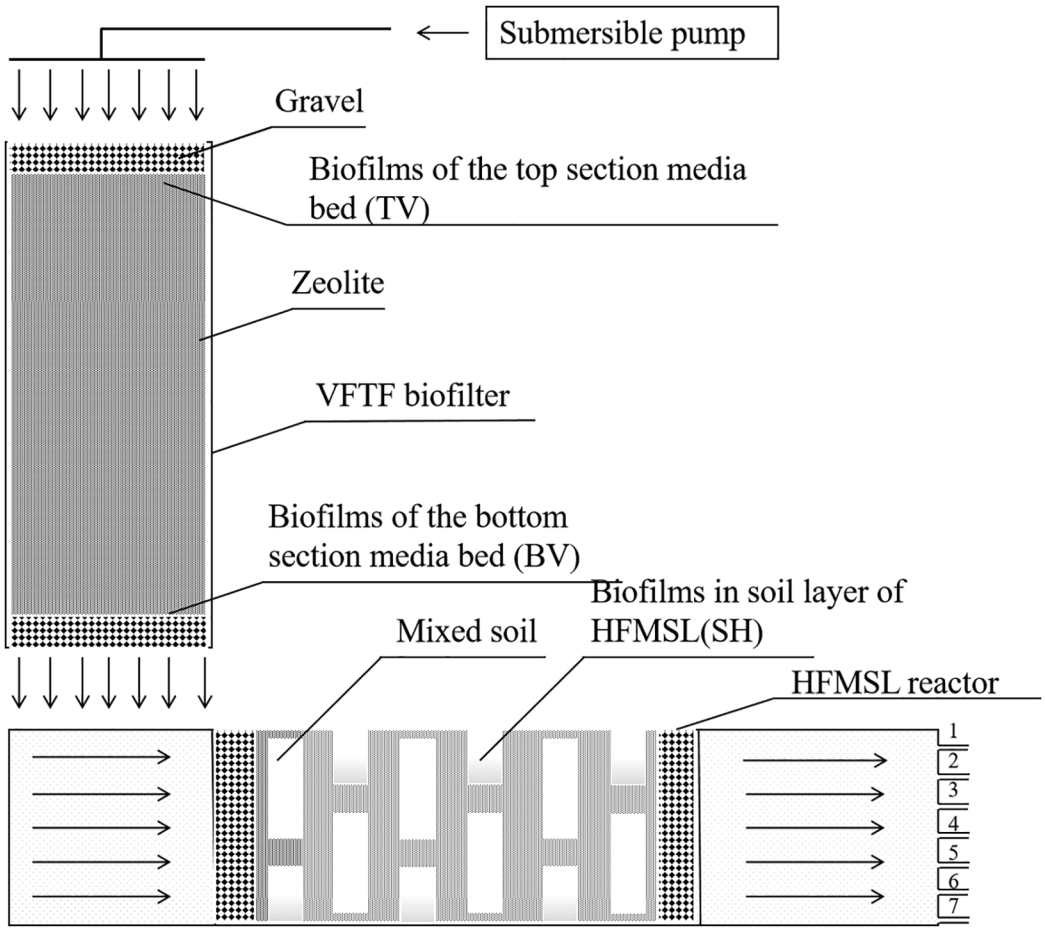

Fig. 1. Schematic diagram of the experimental apparatus. Effluent was discharged only from port 1 when the apparatus was regularly operated, and port 2–7 was used for draining the liquid in HFMSL system when necessary.

microbial community diversity, EPS, and enzymes involved in the inhibition were also investigated in details.

2. Materials and methods

2.1. Experimental apparatus and materials

The VFTF–HFMSL system was built refers to Zhang et al. (2015), and schematic diagram was shown in Fig. 1. Two lidless acrylic boxes filled with different media worked as VFTF and HFMSL respectively. VFTF (320 mm length × 160 mm width × 600 mm height), the vertical one with apertured bottom, which filled with gravel and zeolite (Jinyun, Zhejiang, China). HFMSL (1200 mm length × 160 mm width × 320 mm height), the horizontal one consisted of inlet pool, outlet pool, and MSL bioreactor. The MSL bioreactor in HFMSL included six soil mixture block (SMB) layers surrounded by permeable layers (PL) in brick-like pattern. VFTF was equipped with zeolite, which could benefit microbial growth. Simulated wastewater from the storage tank was pumped intermittently into the system using a submersible pump (YQB-7500, Sensen Group Co. LTD., Zhoushan, Zhejiang, China) which was controlled by a time switch (DJ-D14M, Dingshibao, Shenzheng, China). The pumped water dispersed evenly into VFTF through a set of perforated pipes (R = 10 mm, PVC), and finally gravitated into HFMSL.

The function of each material has been shown in Zhang et al. (2015). Natural zeolite (3–5 mm diameter in VFTF, 1–3 mm diameter in HFMSL) mixed with iron scraps at the ratio of 95:5 by dry weigh. The SMB was the mixture of clayey soil, sawdust and iron scraps and biochar at the ratio of 7:1:1:1 by dry weight. The soil got from the Tianma Mountain (Changsha, China), which passed through a nylon sieve with a size of 20 meshes after being air dried and crushed.

2.2. Influent wastewater quality and operating conditions

According to the actual water quality of rural wastewater, the preparation of simulated wastewater was carried out (Leverenz et al., 2010). Simulated wastewater in experiment was prepared through dissolving starch, glucose, peptone, $NaHCO_3$, NH_4Cl, KH_2PO_4, K_2HPO_4, $MgSO_4$, $CaCl_2$, $MnSO_4$, SDBS (all reagents were analytically pure grade) into 40 L tap water to simulate wastewater in rural area. The system operated for ten phases. In every phase, the reactor ran at influent frequency of water feeding for 1s per 8 min for about 12–20 days until contaminant indicators (COD, NH_4^+-N, NO_3^--N, NO_2^--N, TP) have become stable. The hydraulic loading rate (HLR) was kept at 660 L/m^2/d, and the corresponding nominal hydraulic retention time (HRT) was about 18 h. The influent SDBS concentration in phase 1 to phase 10 was 0, 0.5, 1, 5, 10, 25, 75, 100, 350 and 750 mg/L, respectively. At each phase, the influent NH_4^+-N and TP concentrations were 50 mg/L and 4 mg/L, respectively. The simulated wastewater did not contain NO_3^--N and the COD concentration increased with the concentration of SDBS increased. Specific trace elements ratio was shown in Zhang et al. (2015).

Biofilm was taken from Changsha Guozhen Environmental Protection Technology Co., Ltd. Specific method of biofilm formation was shown Zhang et al. (2015). The water inlet parameters of biofilm formation were the same as phase 1, and the time was about 6 weeks. The maximum, minimum and average ambient temperatures were 30.2 ℃, 22.3 ℃, and 24.6 ℃, respectively. The maximum, minimum and average water temperatures were 23.2 ℃, 16.4 ℃, and 18.6 ℃, respectively.

2.3. Water sampling and analysis

50 mL water samples of influent, mid and final effluent were taken from the storage tank, inlet pool in HFMSL and outlet pool in HFMSL (Fig. 1), respectively. Water samples were taken and analyzed every 2 days. COD, TP, NH_4^+-N, NO_2^--N, NO_3^--N was measured according to the standard methods (APHA, 1998), and pH was measured by pH meter (PHS-3C, INESA Co. Ltd, Shanghai, China). All drugs used in the test were of analytical pure grade.

2.4. Biofilm sampling

Biofilms of the top section media bed of VFTF (TV) and biofilms of the bottom section media bed of VFTF (BV) were taken from top and bottom section media bed VFTF, respectively and biofilms in soil layer of HFMSL (SH) were taken from the soil in HFMSL (Fig. 1), respectively. The biofilm samples were taken at the end of every phase and saved at −80.0 ℃. All biofilm samples were analyzed together after all the 10 phases reaction was completed.

2.5. Separation and three-dimensional fluorescence detection of extracellular polymeric substances (EPS)

Separation of EPS including tightly bound EPS (T-EPS) and loosely bound extra EPS (L-EPS) was by the reference to Li and Yang. (2007). Three-dimensional excitation emission matrix (3D-EEM) was measured by fluorescence spectroscopy (Fluoromax-4 Spectro- fluorometer, HORIBA Scientific, France) with a 450 W Xe arc lamp. Emission (Em) scans and excitation (Ex) wavelengths were performed from 200 to 800 nm and 200 to 600 nm, respectively. Both Ex and Em were at 10 nm intervals as well as 0.05% NaCl solution was recorded as the blank (Luo et al., 2013).

2.6. Key enzymes

According to the moisture content of the sludge, taking 1 g (Dry sludge quality) of wet sludge sample into a 50 mL centrifuge tube and add 5 mL buffer solution to the tube and then ultrasonically broken. Ultrasonic breaker was used with a power of 250 W, an ultrasonic 3 s gap of 5 s and a total length of 5 min. After adding buffer solution, the tube was immersed in an ice bath and stored until the end of the experiment. Ultrasound should also be performed by ice bath. The specific buffer configuration was conFig.d according to the instructions of the enzyme test instructions (Jiancheng, Nanjing, Jiangsu, China).

Amylase (AMS), catalase (CAT), glutathione peroxidase (GSH-Px), superoxide dismutase (SOD), 4 kinds of enzymes were tested, and at the same time concentration of adenosine triphosphate (ATP) and hydrogen peroxide (Px) were also tested. AMS, CAT, GSH-PX, SOD and ATP was detected by iodine liquid colorimetric method, molybdate method, 5,5-Dithiobis (2-nitrobenzoic acid) colorimetric method, hydroxylamine method and phosphomolybdic acid colorimetric method, respectively. The specific test method of all above and Px was based on the assay kit produced by Nanjing Jiancheng and used in accordance with manufacturer's instructions.

2.7. Microbial community change and 16S rRNA functional prediction

6 samples (TV, BB, and SH) in 0 and 750 mg/L of SDBS were sent to Majorbio Bio-Pharm Technology Co., Ltd (Shanghai, China) for high-throughput sequencing. PCR amplification of the 16S rRNA gene was performed for the V3-V4 regions with two specific primers with barcodes (515F-806R). The raw sequences had been submitted to Sequence Read Archive (SRA) database with BioProject PRJNA509408.

Community diversity index and difference analysis were generated using the MOTHUR program and phylogenetic analysis using FastTree software. 16S function prediction using the database of PICRUSt, EggNOG and KEGG.

2.8. Other analytical methods

Volatile suspended solid (VSS) was performed in accordance with

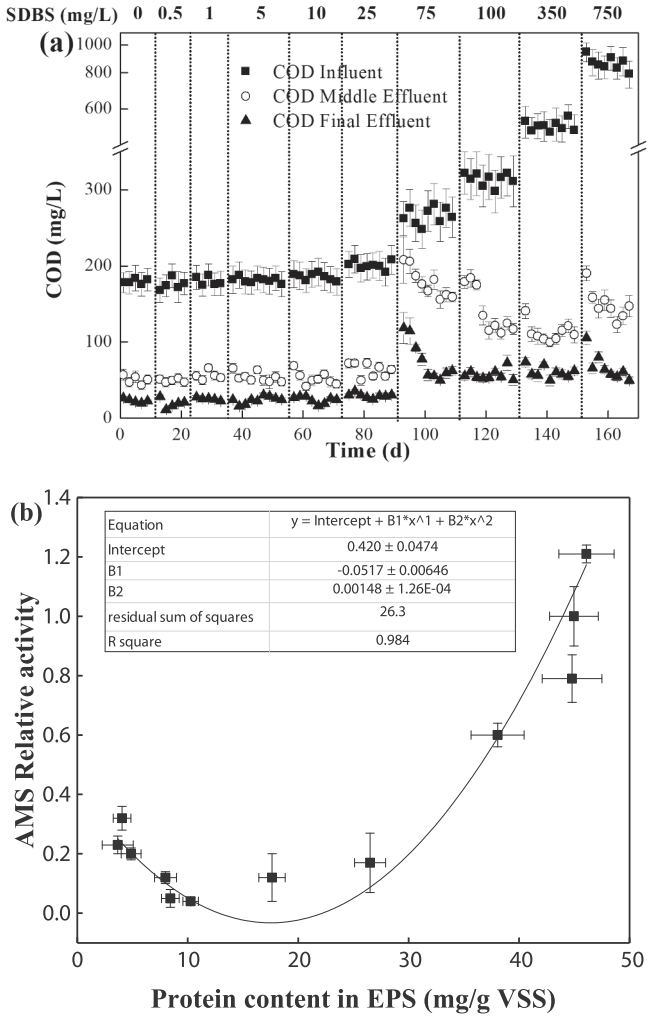

Fig. 2. (a) COD removal performance of the system; (b) A quadratic function model that describes the relationship between the relative activity of amylase and the protein content in EPS.

standard methods (APHA, 1998). The protein and polysaccharides were detected by coomassie brilliant blue G-250 method and anthrone-sulfuric acid method with bovine serum albumin and glucose as standard solution, respectively, specific method refers to previous study (Chen et al., 2017). The drugs used were of analytical pure grade.

2.9. Statistical methods

All tests were conducted in triplicate. An analysis of variance was used to evaluate the significance of results, and $p < 0.05$ was considered to be statistically significant.

3. Results and discussion

3.1. COD removal and carbon source structure changes

3.1.1. Removal of COD and SDBS in the system

Fig. 2a showed the COD value of the original synthetic wastewater, middle effluent, and final effluent at different concentrations of SDBS. As shown in Fig. 2a, the average removal rates of COD in phase 1–6 (< 75 mg/L of SDBS) was 86.3%, and the average final effluent COD concentration steadily kept at 24.4 mg/L in phase 1–6. The average removal rates of COD in phase 7–10 increased with the increase of SDBS concentration, corresponding up to be 71.2%, 81.8%, 88.5% and 92.1%, respectively. Actually, the removal efficiency of COD did not drop and the value of the final effluent was always stable in the long-term run. It was indicated that SDBS had few effects on removal of COD in the system. In this system, the two-stage treatment can ensure the long-term stability of COD effluent. And COD was mainly removed in the VFTF, as part of COD, SDBS was also degraded at the same time. But in the first few days of phase 7, the removal efficiency of COD had dropped significantly in both middle and final, and after adjusting for a period of time, the removal effect of COD was restored to 80.5% and then had kept stable to the end of test. The reason might be the amount of active microorganism in system was too small to degrade the newly added carbon resource (SDBS) in the initial stage. But, with the extension of time, the amount of active microorganism in the system gradually grew, so the removal efficiency of COD was restored and then had kept stable to the end of test (Chen, 2010; Schleheck et al., 2000). However, it was found that the concentration of COD was greater than 50 mg/L at the end of study.

3.1.2. Change of carbon source structure

It was reported that SDBS was first oxidized into small molecules which were the same as the oxidation of fatty acids by α, ω and β oxidation in its long linear chain (Asok and Jisha, 2012; Perez et al., 2000). In early 19th century, Franz Knoop showed that product of β oxidation of fatty acids was acetic acid and which can directly enter the tricarboxylic acid cycle. Therefore, the produced acetic acid easily flowed with the water flow, which affected the subsequent biofilm metabolism of carbohydrate. Since the acetic acid produced in VFTF cannot be monitored, the content of ATP and the activity of amylase (AMS) in different biofilm could be used to explore the carbon source structure (Li et al., 2018; Cheng et al., 2016).

As shown in Fig. 3, The ATP content increased with the increase of SDBS in TV, BV and SH, especially in TV. The highest ATP content was in TV, especially at 350 and 750 mg/L of SDBS. The ATP content in BV and SH was very similar, but even under the condition of 750 mg/L SDBS, the ATP content of BV and SH was only equivalent to the content of TV when carbohydrate was the sole carbon source, which indicate that the decomposition of SDBS was mostly in the top part of VFTF. When the concentration of SDBS was more than 25 mg/L, the activity of AMS was obviously increased in SH, and obviously decreased in BV. It indicated that the metabolism of carbohydrate decreased in BV. This facilitates the entry of carbohydrate into HFMSL as carbon sources of denitrification. It was proved that the direct use of acetic acid could reduce the glycolysis (Li and Yang, 2007). The addition of SDBS did not reduce the activity of AMS in TV immediately, indicating that SDBS itself does not affect the glycolysis. Thus, the reduction in AMS was caused by acetic acid. The decrease in AMS activity of TV occurs after the SDBS concentration was higher than 100 instead of 25 mg/L, which indicate that when the concentration of SDBS was too low, the acetic acid produced by TV was washed by water to BV and when the SDBS concentration was higher than 100 mg/L, the acetic acid produced by TV could be partially used by itself.

It was indicated that the entire glycolytic pathway was total carried out in EPS until pyruvic acid enters the cell for the tricarboxylic acid cycle (Laspidou and Rittmann, 2002; Sung et al., 2018). Glycolysis consists of a series of enzymatic reactions, and most of the enzymes involved in the reaction are proteins. The EPS also changed significantly when using honey as a carbon source (Akker et al., 2011). Therefore, the protein content in EPS should be related to the activity of AMS because there were only two carbon sources, SDBS and carbohydrate in the system. Therefore, it's possible to establish a linear relationship between protein content in EPS and AMS activity. In order to avoid the error caused by the excessive amount of acetic acid produced by SDBS, the EPS protein content of three biofilms with SDBS concentration of 0, 100, 350, 750 mg/L were taken to fit equation with AMS activity. From Fig. 2b, the relationship between protein content in EPS and AMS activity is quadratic function. This relationship should be a general relationship because the microbial composition of the three

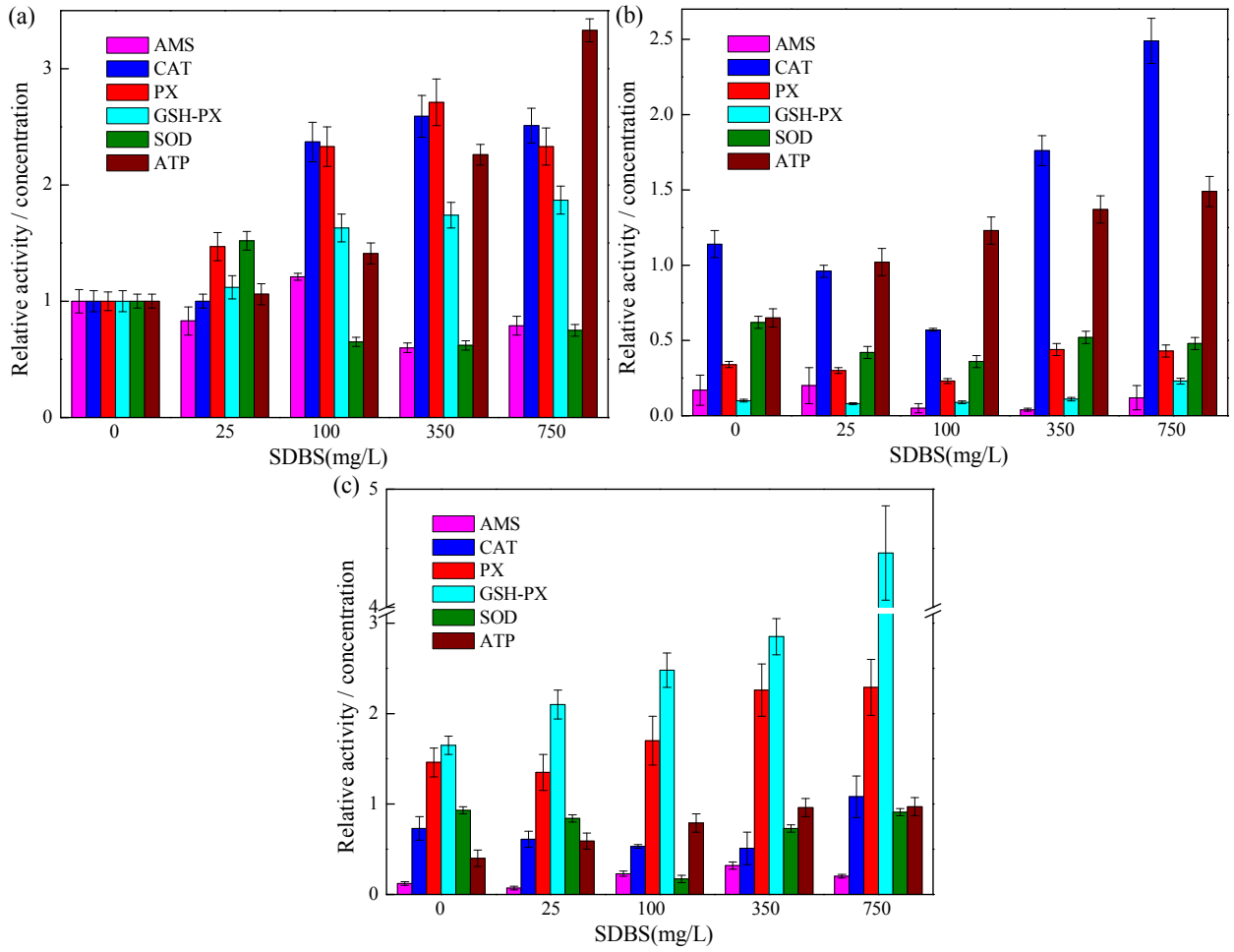

Fig. 3. Key enzymes and important substances in biomass at different concentrations of SDBS. (a) TV; (b) BV; (c) SH. The TV with 0 mg/L SDBS was used as a blank group, and the enzyme activity and Px, ATP concentration were set as 1, and the rest were expressed in multiples of 0 mg/L SDBS.

biofilms was different, and the compositional differences were increasing under the influence of SDBS (This will be analyzed later). Of course, EPS would also change greatly under some stress conditions (such as antibiotics, pesticides, salinity, etc.) (Chen et al., 2018; Wang et al., 2018). These changes may be due to these stress conditions influence on the glycolytic reaction to affect protein content in EPS.

3.2. Nitrification and denitrification in the system and removal of nitrogen and phosphorus

3.2.1. Removal of nitrogen and phosphorus

The influent nitrogen only contained NH_4^+-N with the concentration of 50.0 mg/L. The effect of SDBS on removal of NH_4^+-N in the system was showed in Fig. 4a. From Fig. 4a, it can be observed that the NH_4^+-N concentration in the middle and final effluent was kept at around 20.0 and 10.0–15.0 mg/L, respectively, and kept stable. The removal of NH_4^+-N was limited in HFMSL (mostly around 5 mg/L) because it was difficult for nitrifying bacteria to survive in large quantities in an anaerobic environment.

The change of NO_3^--N concentration was exhibited in Fig. 4b. As shown in Fig. 4b, when the SDBS concentration was 0.50 mg/L, the NO_3^--N concentration had increased from 5.45 to 9.52 mg/L in middle effluent, but the final effluent remained stable due to the buffering effect of the two-stage treatment. As the SDBS concentration reached at 5.00 mg/L, the concentration of NO_3^--N in the middle and final increased significantly, increasing by 10.6 and 8.85 mg/L, respectively. It was suggested that the activity of denitrifying bacteria was severely limited. Whenever the SDBS concentration was changed, the NO_3^--N concentration would rise sharply, and then it would fall back to a stable value. As the acclimation progresses, the stability value was continuously decreasing. The average effluent of the middle and final sections decreased from 15.1 to 8.79 mg/L and 11.6 to 4.74 mg/L. In phase 8–10, the average middle effluent value had remained stable, which was 5.42 mg/L. Therefore, the phase of the denitrifying bacteria acclimation phase to phase 8 had basically ended. The previous study indicated that the higher the C/N in the system, the better the removal of NO_3^--N when using carbonhydrate as a carbon source (Zhang et al., 2015a; Chen et al., 2012). Therefore, the increase of NO_3^--N in Fig. 4b was due to the influence of SDBS rather than C/N. Denitrification was extremely variable with the variation of SDBS.

Since iron scrap was added to the system to absorb phosphorus (Zhang et al., 2015a; He et al., 2018), the TP fluctuates throughout the reaction and remains at a low value around 0.72 mg/L in middle and 0.14 mg/L in final. At the same time, the concentration of NO_2^--N were around 0.28 mg/L (middle) and 0.13 mg/L (final).

3.2.2. Most of the VFTF were still aerobic conditions without an aeration pump

Nitrification is generally considered to be carried out under aerobic conditions, while denitrification and anammox are carried out under anoxic or anaerobic conditions (Chen et al., 2018; Zhang et al., 2015b). However, the VFTF-HFMSL system didn't have an aeration device for convenience in rural areas, which causes an inevitable anaerobic part of the VFTF. Since the influent water was discontinuous, the biofilm of the

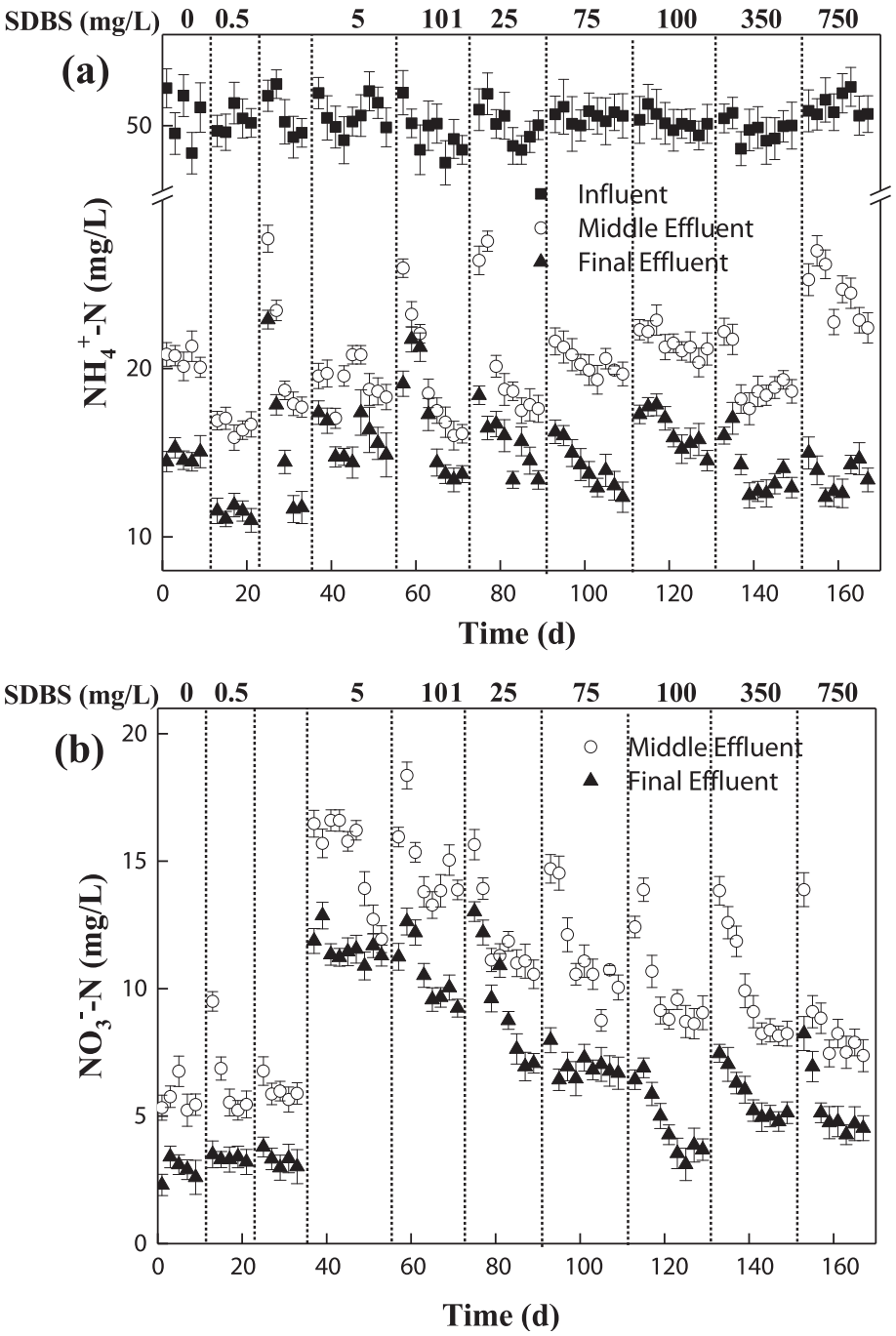

Fig. 4. Removal performance of the system. (a) NH_4^+-N; (b) NO_3^--N.

VFTF would be in direct contact with the air and in that case, the dissolved oxygen in the water cannot directly indicate that the biofilm was aerobic or anaerobic. Therefore, species abundance identification was used to classify the distribution of aerobic and anaerobic bacteria in biofilms.

Fig. 5a showed the top 25 abundance of species were selected on a phylogenetic tree on genus level. Since the phylogenetic tree was classified according to gene similarity, 25 kinds of microorganisms were divided into two regions: prefer aerobic or anaerobic conditions. Most of the microorganisms in TV and BV were aerobic, while SH was anaerobic. However, some of the aerobic and anaerobic microorganisms in Fig. 5a could survive in anoxic state and have a certain effect. Both *Bacilli* and *Rhodobacteraceae* are denitrifying bacteria, but *Bacilli* is an obligate anaerobic bacterium and *Rhodobacteraceae* could use nitrate and nitrite under anoxic conditions (Chen et al., 2018; Sugita et al., 2005). *Bacilli* existed in TV and BV in a small amount, and *Rhodobacteraceae* existed in SH in a small amount. This indicates that some biofilms in VFTF were difficult to access to oxygen. In this environment, *Planctomycetacia* which is anammox bacteria could exist in small amounts (Sugita et al., 2005; Wang and Chen, 2009). Both *Amaricoccus* and *Nakamurella* are obligate aerobic (Ma et al., 2016; Seviour et al., 2000),[38~39] and the large presence of *Nakamurella* indicates that the most part of VFTF was in an aerobic environment. In this way, the VFTF consists of a number of anoxic areas surrounded by the entire aerobic zone. In HFMSL, although the soil and water cannot completely isolate oxygen, the HFMSL was still in an anaerobic environment.

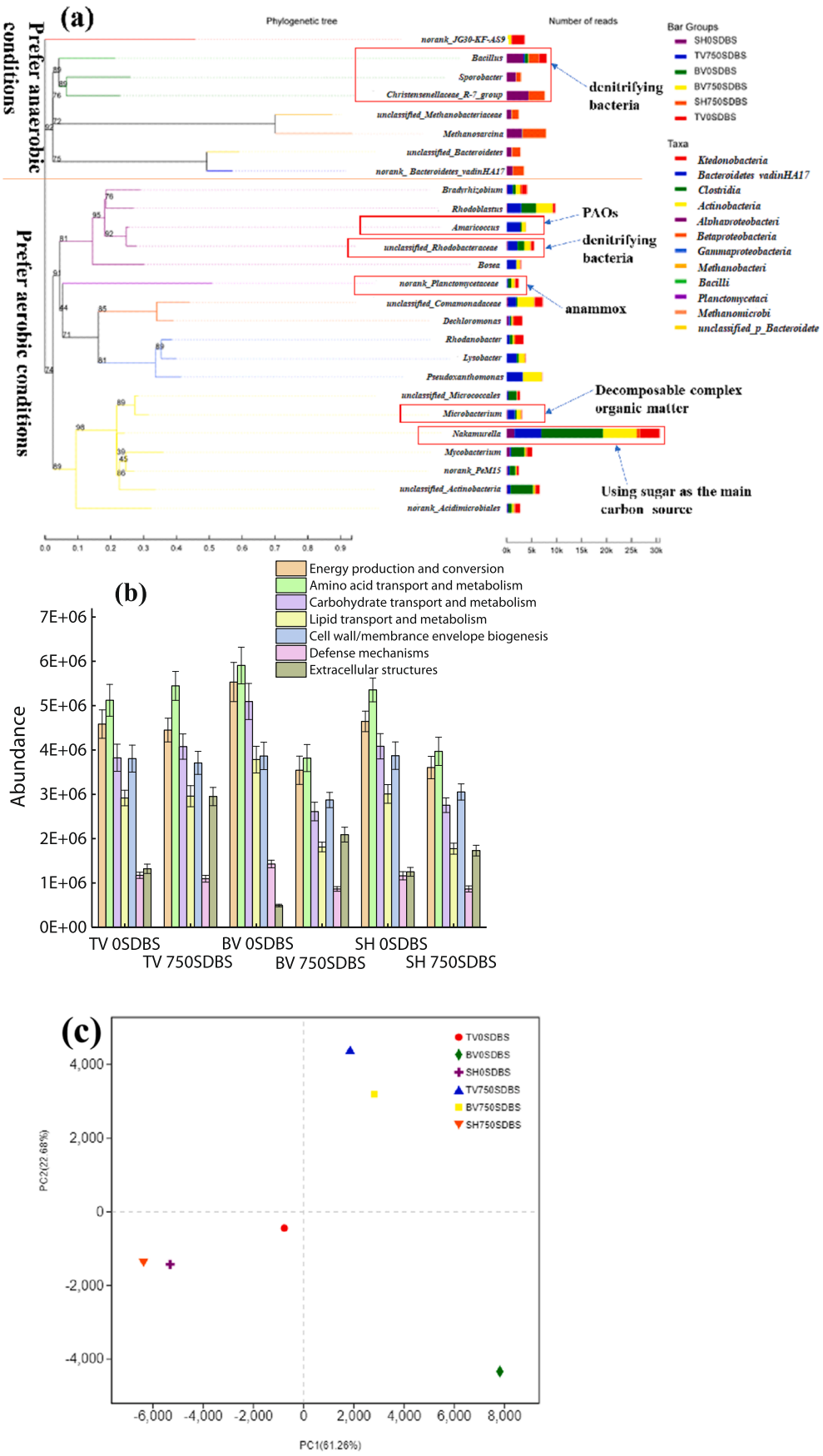

Fig. 5. (a) Phylogenetic tree of 6 activated sludge samples on the genus level; (b) **A**bsolute abundance predicted by 16S function prediction. (c) Beta diversity (Principal component analysis test) on OTU level. (*Note*: the horizontal and vertical coordinates represented the virtual distance of the kinship. The closer the distance between the two points, the closer the kinship is).

3.2.3. Anammox and denitrification worked simultaneously

It can be seen from Fig. 4 that both NH_4^+-N and NO_3^--N removal effect of VFTF was significantly better than that of HFMSL. Even the removal of NO_3^--N in VFTF was better than HFMSL. The denitrifying bacteria abundance in HFMSL was significantly higher than VFTF. However, the abundance of denitrifying bacteria in SH was significantly reduced at 750 mg/L SDBS. In VFTF, *Rhodobacteraceae* abundance increased at 750 mg/L SDBS. This may because some degradation products of SDBS cannot be decomposed under anaerobic conditions, and can be utilized as denitrifying carbon sources under anoxic conditions. The abundance of anammox bacteria did not change much, so the gradual decrease of nitrate nitrogen in the acclimation process in Fig. 4b was due to the fact that denitrifying bacteria gradually adapted to the presence of SDBS. This leads to the conclusion that anammox bacteria in the VFTF determined the lower limit of the TN load, while the activity of the denitrifying bacteria suggested the upper limit of the TN load.

3.3. Biofilm could resist the toxicity of SDBS degradation products after acclimation

3.3.1. Effect of SDBS degradation products on microbial function

It was reported that SDBS has toxic and bioaccumulation effect on many aquatic plants, fish and microorganisms (Parhizgar et al., 2017) and SDBS had an inhibitory effect on denitrifying bacteria was mentioned above. In that way, SDBS indeed has a toxic effect to biofilms, but could biofilms adapt to this condition? RNA in TV, BV, SH was purified, read and functional compared with microbial function database. Fig. 5b showed the functional abundance which changed a lot. It can be seen in Fig. 5b that except for the extracellular structure, the rest of the functions in the TV did not change much. Energy production and conversion and transport and metabolism of carbohydrate, lipid and amino acid were obviously inhibited in BV and SH. This indicated that it's the degradation products of SDBS but not SDBS, which were toxic to biofilms. Carbohydrate, lipid and amino acid are all energy-related, so SDBS degradation products affect the functions of energy production and conversion by affecting these functions related to carbohydrate, lipid and amino acid.

In Fig. 5b, the abundance of extracellular structure of TV, BV and SH all increased in 750 mg/L SDBS, but in the detection of EPS content, only the protein produced a relatively large change. In this case, 3-D EEM was used to characterize EPS. At present, the changes in the 3-D EEM peaks of EPS were mostly compared with the standard peaks of some substance, and the activity of different peaks was hardly measured by the number of shifted peaks (Chen et al., 2015; Lin et al., 2020). A frequent blue or red shift of a fluorescent peak indicates a change in the microstructure of the substance (Andy, 2002; Wu et al., 2018b). Therefore, the more the number of blue shifts and red shift peaks compared to the blank group, the more organic matter represented by the peak is more active. The specific fluorescence peaks were listed in Table 1. The first main peak (peak A) was identified at excitation/emission wavelengths (Ex/Em) of 220–230/310–340 nm, and the second main peak (peak B) was located at 260–280/310–340 nm. The third main peak (peak C) was found at 310–350/370–430 nm. Compared with the sample without SDBS, there are 5, 5, and 9 shifted peaks of A, B, and C, respectively (Table 1). In peak C, only 3 of the 12 control groups did not shift, which indicated that peak C represented some active substances, may be such as some enzymes or coenzymes.

3.3.2. Microbacterium could totally offset the toxicity of SDBS degradation products

On phylum level, *Proteobacteria* was the most abundant microorganism in all biofilms and the abundance increased at a SDBS concentration of 750 mg/L, which indicated that *Proteobacteria* adapted to the presence of SDBS. Fig. 5c showed a principal component analysis (PCA) on OTU level. The microorganism of SH changed little during the entire period. The microorganism changes of TV and BV were very large. At the same time, the SDBS brings the composition of TV and BV closer at 750 mg/L of SDBS. This indicated that VFTF was moving towards SDBS as main carbon source, while HFMSL cannot adapt to SDBS conditions.

The abundance of the other two major microorganisms (*Actinobacteria*, *Firmicutes*) has decreased. In Fig. 5a, the abundance of *Nakamurella* decreases in BV, while *Microbacterium* increases slightly in TV and BV. It was reported that *Nakamurella* mainly used carbohydrate as a carbon source and *Microbacterium* could decompose complex organic matter, such as benzene ring (Ma et al., 2016; Perez et al., 2016). Through the previous analysis, the decrease of *Nakamurella* in BV was caused by the decrease in the dependence of biofilm on carbohydrate. However, *Microbacterium* is a microorganism that was almost non-existent when SDBS wasn't added. A significant increase in the abundance of *Microbacterium* indicated that some substances in the system which difficult to be decomposed were produced in the system. According to the previous analysis, these substances have certain toxic effects on denitrifying bacteria, and the growth of *Microbacterium* relieved the toxicity.

3.3.3. Biofilms alleviate the toxicity of SDBS degradation products by producing some enzymes

Microbacterium can mineralize the toxic substances produced by the degradation of SDBS. Could the remaining microorganisms alleviate the toxicity through the secretion of enzymes? Microorganisms release hydrogen peroxide (PX)-based peroxides to oxidize toxic organic matter in the event of a surge in SDBS. To protect themselves, microorganism would secrete CAT, GSH-PX, SOD (Janknegt et al., 2009; Sabatini et al., 2009; Wang and Chen, 2006). Fig. 3 shows the relative activities of PX, CAT, GSH-PX, and SOD. The same with AMS and ATP, TV samples without SDBS were set as a control group and its relative activity was set as 1. As shown in Fig. 3, activities of PX, GSH-PX, and CAT have significantly improved at 100 mg/L SDBS, and then remain stable in TV. This indicated that at 100 mg/L SDBS, the microorganisms in the TV have adapted to the conditions with SDBS. However, the CAT in BV showed the lowest value at 100 mg/L SDBS, while GSH-PX and PX did not change significantly. This indicated that BV did not receive the toxicity of SDBS degradation production. The peroxide produced by TV flows into BV when the concentration of SDBS was high, resulting in a significant increase in CAT activity. In SH, the activity of PX and GSH-PX increased significantly with the increase of SDBS concentration, and the relative activity was much higher than that of TV and BV. This showed that SH reacts very strongly to SDBS degradation products. However, according to the previous analysis, the abundance of denitrifying bacteria in SH decreased at 750 mg/L SDBS, indicating that these enzymes could only alleviate the toxicity of SDBS degradation products.

4. Conclusions

In general, the VFTF-HFMSL system had a high removal efficiency of SDBS without aeration, but SDBS had a great impact on the function of denitrifying bacteria. Microorganisms capable of decomposing complex organic matter grown obviously in biofilm. At the same time, the remaining microorganisms resisted the toxicity of SDBS by EPS and enzymatic reaction. In biofilm, the protein content in EPS was quadratic with AMS in cells and degradation products of SDBS could inhibit the transport and metabolisms of amino acids, carbohydrates and lipids.

CRediT authorship contribution statement

Wenchang Tang: Investigation, Methodology, Writing-original draft, Validation, Wrting-review & editing. **Xiang Li:** Investigation, Methodology. **Haiyang Liu:** Writing-review & editing, Methodology.

Table 1
The position of each peak in the 3-D EEM diagram. The bold italic and bold underlined digits indicate the red and blue shift of wavelength, respectively and samples of 0 mg/L of SDBS were set as control.

EPS Types	SDBS (mg/L)	Peak A		Peak B		Peak C	
		Ex/Em (nm)	intensity	Ex/Em(nm)	intensity	Ex/Em (nm)	intensity
TV-L-EPS	0	230/330	727	280/330	997	330/420	185
	100	230/330	559	280/330	997	***340/430***	202
	750	***230/340***	375	***280/340***	909	**320/410**	157
BV-L-EPS	0	230/340	850	280/340	889	350/400	159
	100	**230/330**	555	**280/310**	990	***350/410***	459
	750	230/340	629	**270/320**	997	***330/410***	335
SH-L-EPS	0	230/310	639	280/310	907	330/380	315
	100	***230/330***	746	280/310	729	**330/370**	156
	750	***230/330***	960	***280/330***	942	**330/370**	183
TV-T-EPS	0	220/310	891	280/310	816	310/390	228
	100	230/310	998	270/310	825	***330/420***	269
	750	220/310	731	270/310	988	***330/420***	280
BV-T-EPS	0	220/330	997	260/340	987	340/420	275
	100	**230/310**	478	280/340	988	**350/410**	429
	750	230/330	843	**270/310**	999	340/420	369
SH-T-EPS	0	230/310	449	280/310	878	320/380	392
	100	220/310	995	280/310	998	***310/390***	645
	750	230/310	822	280/310	987	***340/390***	342

Shaohua Wu: Methodology. **Qi Zhou:** Formal analysis. **Cheng Du:** Writing-review & editing, Validation. **Qing Teng:** Writing-review & editing. **Yuanyuan Zhong:** Writing-review & editing. **Chunping Yang:** Conceptualization, Project administration, Funding acquisiting, Writing-review & editing.

Declaration of Competing Interest

The authors declare that they have no known competing financial interests or personal relationships that could have appeared to influence the work reported in this paper.

Acknowledgements

Support from the National Natural Science Foundation of China (Grant No.: 51978178, 51478172 and 51521006), the Department of Science and Technology of Guangdong Province of China (Contract No.: 2019A1515012044 and 2018S0011), and the Department of Science and Technology of Hunan Province of China (Contract No.: 2017JJ2029 and 2017SK2362) is highly appreciated.

Appendix A. Supplementary data

Supplementary data to this article can be found online at https://doi.org/10.1016/j.biortech.2019.122634.

References

Akker, B.V.D., Holmes, M., Pearce, P., Cromar, N.J., Fallowfield, H.J., 2011. Structure of nitrifying biofilms in a high-rate trickling filter designed for potable water pre-treatment. Water Res. 45 (11), 3489–3498.
Andy, B., 2002. Fluorescence excitation-emission matrix characterization of river waters impacted by a tissue mill effluent. Environ. Sci. Technol. 36 (7), 1377–1382.
APHA (American Public Health Association), 1998. Standard Methods for the Examination of Water and Wastewater, 20th ed. (Washington, DC, USA). AQ.
Asok, A.K., Jisha, M.S., 2012. Biodegradation of the anionic surfactant linear Alkylbenzene Sulfonate (LAS) by autochthonous *Pseudomonas* sp. Water Air Soil Pollut. 223 (8), 5039–5048.
Bezbaruah, A.N., Tian, C., Zhang, 2010. Quantification of oxygen release by bulrush (*Scirpus validus*) roots in a constructed treatment wetland. Biotechnol. Bioeng. 89 (3), 308–318.
Bundy, C.A., Wu, D., Jong, M.C., Edwards, S.R., Ahammad, Z.S., Graham, D.W., 2017. Enhanced denitrification in downflow hanging sponge reactors for decentralised domestic wastewater treatment. Bioresour. Technol. 226, 1–8.
Chen, Y.J., He, H.J., Liu, H.Y., Li, H.R., Zeng, G.M., Xia, X., Yang, C.P., 2018. Effect of salinity on removal performance and activated sludge characteristics in sequencing batch reactors. Bioresour. Technol. 249, 890–899.
Cheng, Y., He, H.J., Yang, C.P., Zeng, G.M., Li, X., Chen, H., Yu, G.L., 2016. Challenges and solutions for biofiltration of hydrophobic volatile organic compounds. Biotechnol. Adv. 34 (6), 1091–1102.
Chen, W., Westerhoff, P., Leenheer, J.A., Booksh, K., 2015. Fluorescence excitation-emission matrix regional integration to quantify spectra for dissolved organic matter. Environ. Sci. Technol. 37 (24), 5701–5710.
Chen, Y.G., Wang, D.B., Zhu, X.Y., Zheng, X., Feng, L.Y., 2012. Long-term effects of copper nanoparticles on wastewater biological nutrient removal and N_2O generation in the activated sludge process. Environ. Sci. Technol. 46 (22), 12452–12458.
Chen, Q.X., 2010. Acute toxicity of sodium dodecyl benzene sulfonate (SDBS) and sodium dodecyl sulfate (SDS) to the copepod, pseudodiaptomus annandalei. Asian J. Ecotoxicol. 05 (1), 76–82.
Cheng, J.J., Stomp, A.M., 2009. Growing duckweed to recover nutrients from wastewaters and for production of fuel ethanol and animal feed. Clean-Soil Air Water. 37, 17–26.
Fountoulakis, M.S., Daskalakis, G., Papadaki, A., Kalogerakis, N., Manios, T., 2017. Use of halophytes in pilot-scale horizontal flow constructed wetland treating domestic wastewater. Environ. Sci. Pollut. Res. 24, 16682–16689.
He, H.J., Xiang, Z.H., Chen, X.J., Chen, H., Huang, H., Wen, M., Yang, C.P., 2018. Biosorption of Cd (II) from synthetic wastewater using dry biofilms from biotrickling filters. Int. J. Environ. Sci. Technol. 15 (7), 1491–1500.
He, H.J., Chen, Y.J., Li, X., Yan, C., Yang, C.P., Zeng, G.M., 2016. Influence of salinity on microorganisms in activated sludge processes: a review. Int. Biodeterior. Biodegrad. 119, 520–527.
Janknegt, P.J., Graaff, C.M.D., Poll, W.H.V.D., Visser, R.J.W., Rijstenbil, J.W., Buma, A.G.J., 2009. Short-term antioxidative responses of 15 microalgae exposed to excessive irradiance including ultraviolet radiation. Eur. J. Phycol. 44 (4), 525–539.
Laspidou, C.S., Rittmann, B.E., 2002. A unified theory for extracellular polymeric substances, soluble microbial products, and active and inert biomass. Water Res. 36 (11), 2711–2720.
Leverenz, H.L., Haunschild, K., Hopes, G., Tchobanoglous, G., Darby, J.L., 2010. Anoxic treatment wetlands for denitrification. Ecol. Eng. 36 (11), 1544–1551.
Li, X., Yang, W.L., He, H.J., Wu, S.H., Zhou, Q., Yang, C.P., Zeng, G.M., Luo, L., Lou, W., 2018. Responses of microalgae *Coelastrella* sp. to stress of cupric ions in treatment of anaerobically digested swine wastewater. Bioresour. Technol. 251, 274–279.
Li, X.Y., Yang, S.F., 2007. Influence of loosely bound extracellular polymeric substances (EPS) on the flocculation, sedimentation and dewaterability of activated sludge. Water Res. 41 (5), 1022–1030.
Lin, Y., Wu, X., Han, Y., Yang, C.P., Ma, Y., Du, C., Teng, Q., Liu, H.Y., Zhong, Y.Y., 2019. Spatial separation of photogenerated carriers and enhanced photocatalytic performance on Ag_3PO_4 catalysts via coupling with PPy and MWCNTs. Appl. Catal. B: Environ. 258, 117969.
Lin, Y., Wu, S.H., Yang, C.P., Chen, M., Li, X., 2019b. Preparation of size-controlled silver phosphate catalysts and their enhanced photocatalysis performance via synergetic effect with MWCNTs and PANI. Appl. Catal. B: Environ. 245, 71–86.
Lin, Y., Liu, H.Y., Yang, C.P., Wu, X., Du, C., Jiang, L.M., Zhong, Y.Y., 2020... Gamagraphyne as photogenerated electrons transfer layer enhances photocatalytic performance of silver phosphate. Appl. Catal. B: Environ. 264, 118479.
Luo, W., Yang, C.P., He, H.J., Zeng, G.M., Yan, S., Cheng, Y., 2014. Novel two-stage vertical flow biofilter system for efficient treatment of decentralized domestic wastewater. Ecol. Eng. 64 (11), 415–423.
Luo, K., Yang, Q., Li, X.M., Chen, H.B., Liu, X., Yang, G.J., Zeng, G.M., 2013. Novel insights into enzymatic-enhanced anaerobic digestion of waste activated sludge by three-dimensional excitation and emission matrix fluorescence spectroscopy. Chemosphere 91 (5), 579–585.
Ma, S.J., Ding, L.L., Huang, H., Geng, J.J., Xu, K., Zhang, Y., Ren, H.Q., 2016. Effects of

DO levels on surface force, cell membrane properties and microbial community dynamics of activated sludge. Bioresour. Technol. 214, 645–652.
Oakley, S.M., Gold, A.J., Oczkowski, A.J., 2010. Nitrogen control through decentralized wastewater treatment: process performance and alternative management strategies. Ecol. Eng. 36 (11), 1520–1531.
Pant, D., Adholeya, A., 2009. Nitrogen removal from biomethanated spentwash using hydroponic treatment followed by fungal decolorization. Environ. Eng. Sci. 26, 559–565.
Parhizgar, F., Alishahi, A., Varasteh, H., Rezaee, H., 2017. Removing sodium dodecyl benzene sulfonate (SDBS) from aqueous solutions using chitosan. J. Polym. Environ. 25, 836–843.
Perez, M.C., Hornos, F.J.A., Engesser, K.H., Dobslaw, D., Gabalda, C., 2016. Removal of 2-butoxyethanol gaseous emissions by biotrickling filtration packed with polyurethane foam. N. Biotechnol. 33 (2), 263–272.
Perez-Armendariz, B., Moreno, Y.M., Monroy-Hermosillo, O., Guyot, J.P., Gonzalez, R.O., 2010. Anaerobic biodegradability and inhibitory effects of some anionic and cationic surfactants. Bull. Environ. Contam. Toxicol. 85 (3), 269–273.
Sabatini, S.E., Juárez, A.B., Eppis, M.R., Laura, B., Luquet, C.M., 2009. Oxidative stress and antioxidant defenses in two green microalgae exposed to copper. Ecotoxicol. Environ. Saf. 72 (4), 1200–1206.
Schleheck, D., Dong, W., Denger, K., Heinzle, E., Cook, A.M., 2000. An *alpha-proteobacterium* converts linear alkylbenzenesulfonate surfactants into sulfophenylcarboxylates and linear alkyldiphenyletherdisulfonate surfactants into sulfodiphenylethercarboxylates. Appl. Environ. Microbiol. 66 (5), 1911–1916.
Seviour, R.J., Maszenan, A.M., Soddell, J.A., Tandoi, V., Patel, B.K.C., Kong, Y.H., Schumann, P., 2000. Microbiology of the 'G-bacteria' in activated sludge. Environ. Microbiol. 2 (6), 581–593.
Sung, T.O., Kang, S.J., Azizi, A., 2018. Electrochemical communication in anaerobic digestion. Chem. Eng. J. 353, 878–889.
Sugita, H., Nakamura, H., Shimada, T., 2005. Microbial communities associated with filter materials in recirculating aquaculture systems of freshwater fish. Aquaculture 243, 403–409.
Wang, D.B., Duan, Y.Y., Yang, Q., Liu, Y.W., Ni, B.J., Wang, Q.L., Zeng, G.M., Li, X.M., Yuan, Z.G., 2018. Free ammonia enhances dark fermentative hydrogen production from waste activated sludge. Water Res. 133, 272–281.
Wang, L.M., Zheng, Z., Luo, X.Z., Zhang, J.B., 2011. Performance and mechanisms of a microbial-earthworm ecofilter for removing organic matter and nitrogen from synthetic domestic wastewater. J. Hazard. Mater. 195 (195), 245–253.
Wang, J.L., Chen, C., 2009. Biosorbents for heavy metals removal and their future. Biotechnol. Adv. 27 (2), 195–226.
Wang, J.L., Chen, C., 2006. Biosorption of heavy metals by *Saccharomyces cerevisiae*: a review. Biotechnol. Adv. 24 (5), 427–451.
Wu, S.H., He, H.J., Li, X., Yang, C.P., Zeng, G.M., Wu, B., He, S.Y., Li, L., 2018a. Insights into atrazine degradation by persulfate activation using composite of nanoscale zero-valent iron and graphene: performances and mechanisms. Chem. Eng. J. 341, 126–136.
Wu, S.H., Li, H.R., Li, X., He, H.J., Yang, C.P., 2018b. Performances and mechanisms of efficient degradation of atrazine using peroxymonosulfate and ferrate as oxidants. Chem. Eng. J. 353, 533–541.
Wu, M.Y., Li, K.B., 2002. Advances in research on treatment of surfactant pollution. Nat. Mag. 24 (3), 138–141.
Yang, C.P., Qian, H., Li, X., Cheng, Y., He, H.J., Zeng, G.M., Xi, J.Y., 2018. Simultaneous removal of multicomponent VOCs in biofilters. Trends Biotechnol. 36 (7), 673–685.
Ying, Q.F., Xiao, C.S., Ji, S.L., Lin, S.Z., 2002. The biodegradation of linear alkylbenzenesulphonate (LAS). Microbiol. China 29, 85–89.
Zhang, Y., Cheng, Y., Yang, C.P., Luo, W., Zeng, G.M., Lu, L., 2015a. Performance of system consisting of vertical flow trickling filter and horizontal flow multi-soil-layering reactor for treatment of rural wastewater. Bioresour. Technol. 193, 424–432.
Zhang, Y., Ma, J., Zhou, S.Y., Ma, F., 2015b. Concentration-dependent toxicity effect of SDBS on swimming behavior of freshwater fishes. Environ. Toxicol. Pharmacol. 40 (1), 77–85.
Zhou, Q., Li, X., Lin, Y., Yang, C.P., Tang, W.C., Wu, S.H., Li, D.H., Luo, W., 2019. Effects of copper ions on removal of nutrients from swine wastewater and on release of dissolved organic matter in duckweed systems. Water Res. 158, 171–181.
Zhou, Q., Lin, Y., Li, X., Yang, C.P., Han, Z.F., Zeng, G.M., Lu, L., He, S.Y., 2018. Effect of zinc ions on nutrient removal and growth of *Lemna aequinoctialis* from anaerobically digested swine wastewater. Bioresour. Technol. 249, 457–463.